Int. J. Electrochem. Sci., 8 **(2013)** 10498 - 10505

International Journal of
ELECTROCHEMICAL
SCIENCE
www.electrochemsci.org

Deposition of Nanocrystal Co_3O_4 on Graphene Nanosheets as Anode Materials for Lithium Ion Batteries

Shan Fan[1,2],*Yong Zhang* [1,2,*],*Xiangang Ma*[3],*Eryun Yan*[1], *Xijun Liu*[1,2], *Shuhua Li*[1], *Wenchao Liang*[1], *Xiaodong Zhai*[1]

[1] College of Material Science and Engineering, Qiqihar University, Qiqihar 161006, People's Republic of China
[2] Key Laboratory of Polymer Composition and Modification, College of Heilongjiang Province
[3] Dalian Institute of Chemical Physics, Chinese Academy of Sciences
[*]E-mail: fanshan33@aliyun.com

Received: 22 April 2013 / *Accepted:* 2 July 2013 / *Published:* 1 August 2013

We report a facile strategy to synthesize the nanocomposite of Co_3O_4 nanoparticles anchored on conducting graphene as an advanced anode material for high-performance lithium-ion batteries. The nanocomposite was characterized by X-ray diffraction (XRD), X-ray photoelectron spectroscopy (XPS), scanning electron spectroscopy (SEM) and transmission electron microscopy (TEM). It was found that the Co_3O_4 nanoparticles obtained are 10-30 nm in size and homogeneously anchor on graphene sheets as spacers to keep the neighboring sheets separated. The electrochemical properties of this Co_3O_4/grapheme nanocomposite as an anode material for lithium-ion batteries is evaluated. The nanocomposite displays superior Li-battery performance with the high capacity, superior rate capability, and excellent cyclic stability.

Keywords: Cobalt oxide, Graphene, Nanocrystalline materials, Lithium-ion battery

1. INTRODUCTION

Lithium-ion batteries have been receiving considerable attention for avariety of applications in consumer electronics and electric vehicles [1-3]. The energy and the power density of the Li-ion battery strongly depend on the properties of cathode and anode materials. Among them, Co_3O_4 attracts extensive interest for lithium-ion batteries (LIBs) due to its high theoretical capacity (890 mAh $\cdot g^{-1}$), more than two times larger than that of graphite (372 mAh $\cdot g^{-1}$), which are expected to meet the requirements of future energy storage systems [4-6]. However, its large volume expansion/contraction and severe particle aggregation associated with the Li^+ insertion and extraction process lead to

electrode pulverization and loss of interparticle contact and, consequently, result in a large irreversible capacity loss and poor cycling stability[7-8]. A variety of appealing strategies have been utilized to solve these intractable problems, including the use of carbon-based nanocomposites [9-10] and unique Co_3O_4 nanostructures of the shape, size, and interparticle spacing of the assembly [11-14]. However, to keep large reversible capacity combined with high Coulombic efficiency, achieving long cycling life and good rate capability of Co_3O_4 electrode material still remains a challenge.

Graphene, a two-dimensional monolayer of sp^2-hybridized carbon atoms, is recently expected to be an advanced anode material in LIB [15-17] due to its extraordinary electrical properties, unusual mechanical strength, and ultralarge specific surface area [18-20]. Theoretically, a singlelayer GN offers a Li-storage capacity of 744 mAh g^{-1} if Li ions are attached to both sides of the graphene sheets. It has been demonstrated that GN-based anode materials exhibit large initial discharge capacity and reversible capacity, although they suffer from large irreversible capacity, low initial Coulombic efficiency, and fast capacity fading [16-20]. Because the ultrathin flexible graphene layers not only can provide a support for anchoring well-dispersed NPs and work as a highly conductive matrix for enabling good contact between them, but also can effectively prevent the volume expansion/ contraction and aggregation of NPs during Li charge/discharge process [18-20].More importantly, graphene can also be used in composites with metallic or oxide NPs to improve the electrochemical performance of these particles.

In this Article, we report a facile strategy for the anchoring of Co_3O_4 nanoparticles on GNs as an advanced anode material for high-performance LIBs. The Co_3O_4 NPs obtained are 10-30 nm in size and homogeneously anchor on grapheme sheets as spacers to keep the neighboring sheets separated. This Co_3O_4/graphene nanocomposite displays superior LIB performance with large reversible capacity, high coulombic efficiency, excellent cyclic performance, and good rate capability, highlighting the importance of the anchoring of NPs on graphene sheets for maximum utilization of electrochemically active Co_3O_4 NPs and graphene for energy storage applications in high-performance LIBs.

2. EXPERIMENTAL SECTION

2.1 Synthesis of Co_3O_4 /graphene nanocomposite

Graphite oxide (GO, 20 mg), synthesized by a modified Hummer's method [21], was ultrasonically dispersed in a *N*,*N*-dimethylformamide (DMF)/ water (10:1 in volume) mixed solvent for 1 h. 1 mmol $Co(NO_3)_2 \cdot 6H_2O$, followed by ammonia solution ($NH_3 \cdot H_2O$, 25 wt %), was slowly added into the above suspension and then stirred for several hours to ensure complete reaction. Then the mixture was transferred into a Teflon-lined stainless steel autoclave and maintained at 180 ºC for 24 h. The obtained composite precursor was filtered and dried under vacuum at 80 °C. Finally, the composite precursor was calcined at 550 °C in air for 2 h to obtain the Co_3O_4/graphene composite. For comparison, bare Co_3O_4 was prepared using the similar procedures without adding GO.

2.2 Materials Characterization

X-ray diffraction (XRD) patterns of the products were collected on a Stoe STADI powder diffractometer equipped with Cu Kα radiation. X-ray photoelectron spectroscopy (XPS) analysis was performed on a Escalab 250, spectrometer with a monochromatic Al Kα radiation. The microstructures were observed by field emission scanning electron microscopy (FE-SEM) on a S5500 microscope and transmission electron microscopy (TEM) on a JEM 2100F microscope.

2.3 Electrochemical Measurements

The working electrodes were prepared by mixing 80 wt % active material (Co_3O_4/graphene, Co_3O_4), 12 wt % acetylene black, and 8 wt% polyvinylidene fluoride (PVDF, 5 wt%) binder dissolved in *N*-methyl-pyrrolidinone. After coating the above slurries on Cu foils, the electrodes were dried at 130 °C in vacuum for 8 h to remove the solvent before pressing. Then the electrodes were cut into disks (12 mm in diameter) and dried at 110 °C for 8 h in vacuum. For graphene, the electrode was prepared by the same procedure with 70 wt % graphene, 10 wt % acetylene black, and 20 wt % PVDF. Electrochemical measurements were carried out *via* CR2025 (3V) coin-type cell with lithium metal as the counter/reference electrode, Celgard 2400 membrane separator, and 1 M $LiPF_6$ electrolyte solution dissolved in a mixture of ethylene carbonate (EC) and dimethyl carbonate (DMC) (EC/DMC, 1:1 v/v). The cells were assembled in an argon-filled glovebox. CV measurements were carried out using a Solartron 1287 electrochemical workstation at a scanning rate of 1 mVs^{-1}. Galvanostatic charge_discharge cycles were tested by LAND CT2001A electrochemical workstation at various current densities of 50~500 mA g^{-1} between 3 and 0.01 V (vs. Li^+/Li) at room temperature.

3. RESULTS AND DISCUSSION

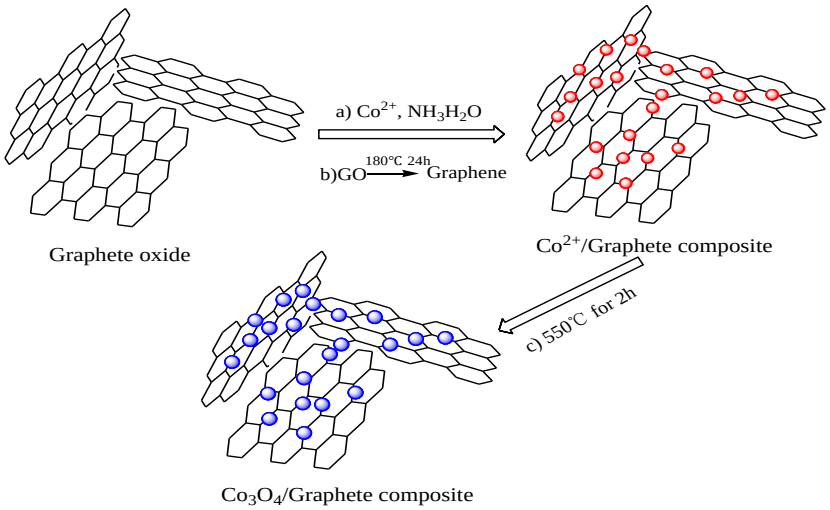

Figure 1. Schematic representation of the fabrication process of Co_3O_4/graphene composite.

The scheme for fabricating Co_3O_4/GN composite consists of three steps: (a) Solution-phase dispersion of Co^{2+} inorganic salt on graphene oxide sheets in basic ($NH_3 \cdot H_2O$) aqueous solution. (b) The graphene oxide was reduced to grapheme and subsequent formation Co^{2+}/grapheme composite. (c) Transformation of Co^{2+}/grapheme composite into Co_3O_4/graphene composite by calcination at 550 °C, as illustrated in Figure 1.

The XRD patterns of the Co_3O_4/grapheme and Co_3O_4 are shown in Figure 2a-2b. Composite of the both, an additional small and low broad (002) diffraction peak appears at 2θ of 26-27.5°, which can be indexed into the disorderedly stacked graphene sheets. Moreover, this broad peak is weaker than that of the as-prepared grapheme (Figure 2c), suggestive of more disordered stacking and less agglomeration for graphene sheets in composite [21, 22].

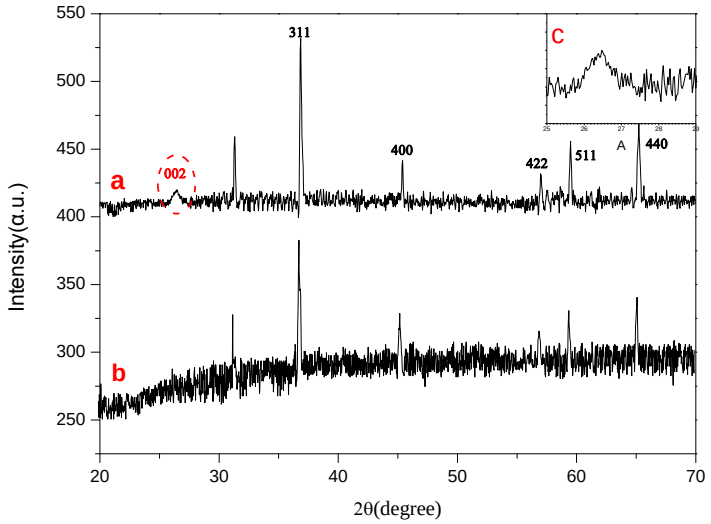

Figure 2. (a) XRD patterns of Co_3O_4/graphene composite, (b) XRD patterns of bare Co_3O_4, (c) The low and broad (002) diffraction peak at 2θ of 25−29° indicates the disordered stacking nature of graphene sheets

To determine the chemical composition of Co_3O_4/graphene composite, X-ray photoelectron spectroscopy (XPS) measurements were carried out (Fig. 3a). The Co 2p XPS spectra of the composite exhibit two peaks at 795.58 and 780.68 eV, corresponding to the Co $2p_{1/2}$ and Co $2p_{3/2}$ spin-orbit peaks of Co_3O_4 (Figure 3b). The presence of Co_3O_4 can be further confirmed by the O 1s XPS peak at 530.6eV, which corresponds to the oxygen species in the Co_3O_4 phase (Figure 3c) [1, 15]. Corresponding to carbon atoms in graphene, The sp^2 carbon peak (284.1 eV)observed is related to graphitic carbon in graphene, and the small O1s peak (530.2 eV) is in the spectrum indicates the presence of residual oxygencontaining groups (such as -OH and O-C=O,) bonded with C atoms in graphene (Figure 3c).It is important to note that the C/O ratio for graphene in the composite was estimated to be 55.0 after subtracting the oxygen species involved in O-Co chemical bonds of Co_3O_4 in the composite, which is much higher than that (10.7) of the as-prepared graphene. It is considered that the decreased oxygen-containing groups are possibly involved in the formation of Co_3O_4 anchored on

the surface of graphene sheets, and a further study is required to elucidate this point in the future. Such a high C/O ratio of the graphene sheets implies a good electronic conductivity, which may enable the graphene sheets to serve as the conductive channels between Co_3O_4 NPs, and is favorable for stabilizing the electronic and ionic conductivity consequently.

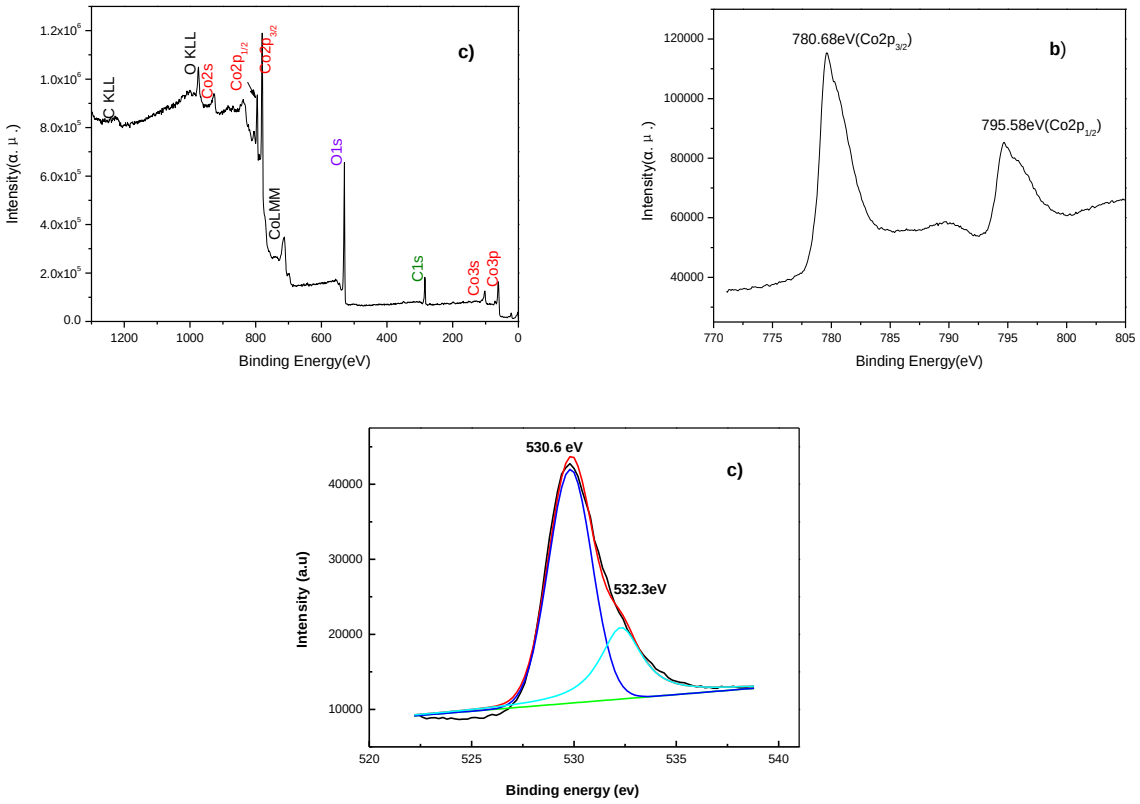

Figure 3. XPS spectrum (a) of Co_3O_4/grapheme composite.Co 2p (b) and O 1s (c) XPS spectra of Co_3O_4/grapheme composite.

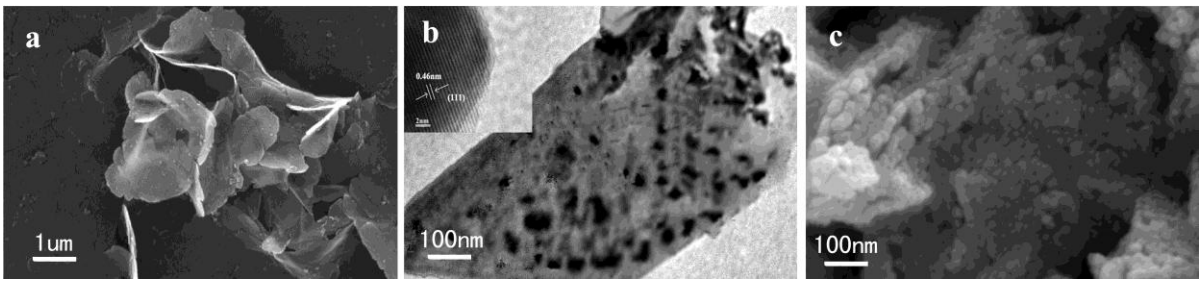

Figure 4. (a) SEM, (b)TEM images of Co_3O_4/grapheme，the inset in (b) is the HR-TEM images of Co_3O_4/grapheme, and (c)SEM images of bare Co_3O_4.

The SEM and TEM images of the Co_3O_4 NPS and Co_3O_4/graphene composite are presented in Figure 4, respectively. As one can see from Figure 4a, small Co_3O_4 NPs are closely anchored on the surface of graphene sheets undergone vigorous sonication, implying a strong interaction between graphene and Co_3O_4. The Co_3O_4 NPS (10-30nm) can be seen homogeneously anchored on the thin

graphene layers from the TEM images (Figure 4b). The HRTEM images of an individual Co_3O_4 particle on graphene (inset in Figure 4c) clearly demonstrate the well-textured Co_3O_4 NPs in the Co_3O_4/grapheme composite, consistent with the XRD results. The fringe spacing is measured to be 0.46 nm, corresponding to the interplanar spacing of (111) plane of Co_3O_4. It should be emphasized that, without the presence of graphene, no Co_3O_4 NPs were formed at the same conditions as those for the preparation of the Co_3O_4/graphene composite in Figure 4c.

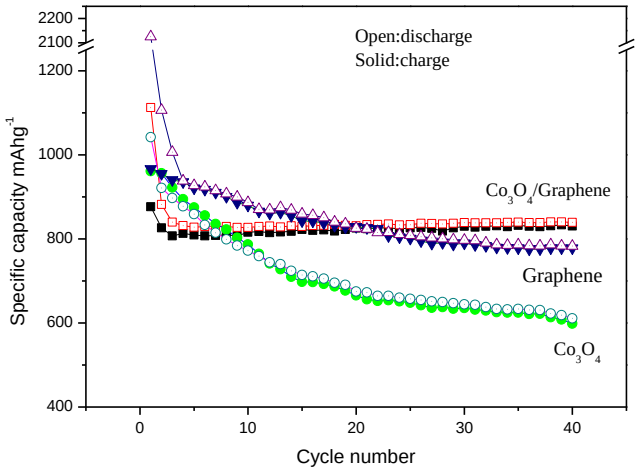

Figure 5. Comparison of the cycling performance of graphene, Co_3O_4, and the Co_3O_4/graphene composite.

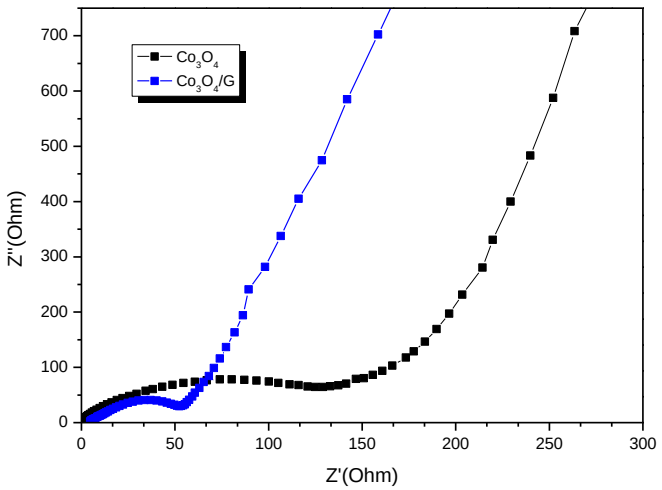

Figure 6. Nyquist plots of Co_3O_4/G and bare Co_3O_4 electrodes after 10 cycles

From Figure 5, the Co_3O_4/graphene composite exhibits a much better cycling performance than graphene and Co_3O_4. It can be seen that the reversible capacity of graphene and Co_3O_4 decreases from 961 to 778.3 mAh g^{-1} and from 961 to only 598.3 mAh g^{-1}, respectively, up to 30 cycles. In contrast, the reversible capacity of the Co_3O_4/graphene composite slightly increases with cycling and reaches ~

839.6 mAh g^{-1} after 30 cycles. It is important to note that there is a strong synergistic effect between Co_3O_4 NPs and grapheme sheets in the composite, which becomes much more apparent with cycling and plays a central role in the excellent cyclic performance of the Co_3O_4/grapheme composite.

EIS measurements were carried out to understand the effect of graphene on the electrochemical behaviors of Co_3O_4. Fig.5 gives the Nyquist plots of the Co_3O_4 and Co_3O_4/G composites after 10 charge-discharge cycles. The plots are composed of two partially overlapped semicircles at high- and medium-frequency ranges and a sloping line at the low frequency range. The high-frequency semicircle corresponds to the solid electrolyte interface (SEI) layer resistance R_{SEI}; the middle-frequency semicircle is related to the charge transfer resistance R_{ct}; the sloping line at the low frequency is associated with the Li-ion solid phase diffusion in the bulk electrode. The Co_3O_4/G electrode shows smaller R_{SEI} and R_{ct} than the bare Co_3O_4 electrode. The better wetting the active material and refrained particles aggregation are responsible for the low R_{ct} value for Co_3O_4/G. The stabilization of the electrode by confining the active particles between the graphene sheets is considered to account for its low R_{SEI} value. A lower R_{ct} for Co_3O_4/G can explain its good cycling stability and rate capability. In addition, a low R_{SEI} value is also beneficial for the reversible cycling of the electrode. As a result, the EIS measurements agree well with the different electrochemical behaviors of Co_3O_4 with and without graphene.

4. CONCLUSIONS

In summary, we have developed a two-step process to synthesize Co_3O_4-graphene nanocomposites. The nanoparticles with an average size of 10-30 nm are uniformly anchored on graphene. The nanocomposite shows improved electrochemical properties compared to the bare oxide. The resulting Co_3O_4@GN hybrid anode thus exhibited superior Li-ion performance with high reversible capacity, excellent cycleability, and good rate capability. This improved performance could be attributed to the formation of 2D GN framework decorated with well-dispersed Co_3O_4 nanocrystals, thus inducing fast diffusion of Li ions and low internal resistance.

ACKNOWLEDGEMENTS
The authors acknowledge financial support from the Key Subject of Departement of Education of Heilongjiang Province (No.12531773) and the Program for Young Teachers Scientific Research in Qiqihar University (2011k-M25).

References

1. Z. S. Wu, W.C. Ren, L. Wen, L.B. Gao, J.P. Zhao, Z.P. Chen, et al. *ACS Nano.* 4 (2010) 3187.
2. L. H. Hu, Q. Peng, Y.D. Li. *J.Am. Chem. Soc*. 130 (2008) 16136.
3. C. Liu, F. Li, L.P. Ma, H.M. Cheng, *Adv. Mater.* 22 (2010) 28.
4. Y. G. Li, B. Tan, Y.Y. Wu. *J. Am. Chem. Soc* 128 (2006) 14258.
5. Yang H, Hu Y, Zhang X, Qiu G. *Mater. Lett*. 2004, 58:378-383.
6. H.Hu, B.Yang, J.Zeng, Y.Qian. *Mater. Chem.Phys.* 86(2004) 233.

7. E. L. Salabas, A. Rumplecker, F. Kleitz, F. Radu, F. Schuth. *Nano Lett.* 6 (2006) 2977.
8. S. L. Xiong, C.Z. Yuan, M.F. Zhang, B.J. Xi, Y.T. Qian. *Chem.Eur. J.* 15 (2009) 5320.
9. R Xu, H.C. Zeng. *Langmuir* 20 (2004) 9780.
10. K.M. Sumanta, R. J Ranga. *Phys. Chem.* C 115 (2011) 2554.
11. Y. H. Tenga, S. Yamamotob, Y. Kusanoc, M. Azumaa, Y. Shimakawa. *Mater. Lett.* 64 (2010) 239.
12. X. Zhao, B.M. Sanchez, P.J. Dobson, P.S. Grant. *Nanoscale* 3 (2011) 839.
13. S. Fan, X.J. Liu, Y.F. Li, E.Y. Yan, C.H. Wang, J.H. Liu, Y. Zhang. *Mater. Lett* 91 (2013) 291.
14. A. Rumplecker, F. Kleitz, E.L. Salabas, F. Schüth. *Chem.Mater*. 2007, 19: 485-496.
15. S. Y. Liu, J. Xie, Q. Pan, C.Y. Wu, G.S. Cao, T. J. Zhu, X.B. Zhao. *Int. J. Electrochem. Sci*. 7 (2012) 354.
16. P. Lian, X.Zhu, S.Liang, Z.Li, W.Yang, H.Wang. *Electrochim. Acta* 55 (2010) 3909.
17. B. J. Li, H .Q. Cao, J. Shao, G. Q. Li, M. Z. Qu, and G. Yin, *Inorg. Chem.* 50 (2011) 1628.
18. O. Oloniyo, S. Kumar, K. Scott, *J. Electron. Mater.* 41 (2012) 921.
19. Z. H. Fu, X.J. Lin, T. Huang, A.S. Yu, J. Solid State Electrochem., 16 (2012) 1447.
20. D. Y Pan, S.Wang, B.Zhao, M. H.Wu, H. J.Zhang, Y.Wang, Z.Jiao. *Chem. Mater*. 21(2009) 3136.
21. W. S. Hummers and R. E.Offeman, *J. Am. Chem. Soc.* 80 (1958) 1339.
22. X. C. Dong, H. X. Xue, W.Wang, Y.X. Huang, B. Mary, C.Park, et al. *ACS Nano*. 6 (2012) 3206

© 2013 by ESG (www.electrochemsci.org)